

## Infrared passbands from fractal slit patterns on a metal plate

Weijia Wen,<sup>a)</sup> Z. Yang, Gu Xu, Yonghai Chen, Lei Zhou, Weikun Ge, C. T. Chan, and Ping Sheng

*Department of Physics and Institute of Nano Science and Technology, Hong Kong University of Science and Technology, Clear Water Bay, Kowloon, Hong Kong, China*

(Received 26 March 2003; accepted 21 July 2003)

We show that a fractal pattern of submicron wide slits, etched on a 0.1- $\mu\text{m}$ -thick gold film, exhibit multiple pass and stop bands in the wavelength regime of 2–200  $\mu\text{m}$ . In the midinfrared regime, the passbands show  $\sim 36\%$  transmission (three orders of magnitude higher than the reference), and the stop bands exhibit  $\sim 80\%$  reflection. In the far infrared regime, the passband transmittances are 25%, 29%, and 14%, respectively, at wavelengths of 34, 62, and 111  $\mu\text{m}$ . These transmittances are rather high in view of the fact that supporting substrate is itself only about 40% transmitting, and a control pattern of holes with similar void-to-metal ratio is 3000 times less transmitting in all frequencies. We attribute the high transmittance from subwavelength slits to geometric resonances. © 2003 American Institute of Physics. [DOI: 10.1063/1.1611271]

Spectral bands can be induced by either Bragg scattering or localized resonances. Whereas the former requires periodicity, the latter can result from nonperiodic structures with features smaller than the relevant wavelengths.<sup>1–4</sup> Microwave transmission through subwavelength slits due to Fabry–Pérot resonances have been demonstrated both theoretically and experimentally.<sup>5–8</sup> Remarkable visible optical transmission through the subwavelength periodic two-dimensional metallic holes has been reported recently and the optical transparency is traced to the coupling of light and surface plasmons of metal plate.<sup>9,10</sup> In this work, we show that a fractal pattern of subwavelength slits exhibits pass and stop bands in the IR regime. The transmittance in the passbands can be very high, even though the slits are very narrow compared with the wavelength. The fractal slit patterns are etched on 0.1- $\mu\text{m}$ -thick gold film, supported by a 400- $\mu\text{m}$ -thick Si wafer, to induce infrared pass and stop bands in the wavelength regime of 2–200  $\mu\text{m}$ . (The standalone Si wafer has about 40% transmittance in all frequencies considered.) Whereas the passbands show  $\sim 36\%$  transmission (three orders of magnitude higher than the reference), the stop band(s) exhibits  $\sim 80\%$  reflection, with a transmission 70 times lower than the passband. In the far infrared regime, the plate yields 25%, 29%, and 14% transmittances at passband wavelengths of 34, 62, and 111  $\mu\text{m}$ , respectively, and 0.5% at the stop band of 21.7  $\mu\text{m}$ . The high transmission from the subwavelength slits is due to the geometric resonance induced by the fractal slit pattern, and is quite different from the surface plasmon coupled tunneling of evanescent waves observed in periodic patterns.<sup>9,10</sup>

For the fabrication of the infrared samples on a 400- $\mu\text{m}$ -thick silicon wafer, the desired fractal pattern was converted onto the photoresist, on which Ti and Au were then deposited with thicknesses of 5 and 100 nm, respectively. Stripping the exposed photoresist leaves the slits (0.5  $\mu\text{m}$  in width) with a deterministic space-filling-curve pattern formed on the gold film, forming an “inverse fractal” configuration. A scanning

electron microscopy (SEM) picture for the inverse metallic fractal can be seen in Fig. 1, where the dimension of the fractal is  $55.6 \times 55.6 \mu\text{m}^2$ , with nine levels of the fractal patterns can be seen in (a) and the enlarged part of Fig. 1(a) is seen in Fig. 1(b), where the 0.5  $\mu\text{m}$  slits can be seen very clearly. The sample measured in our experiment, with a dimension of  $15 \times 15 \text{ mm}^2$ , was composed of periodically du-

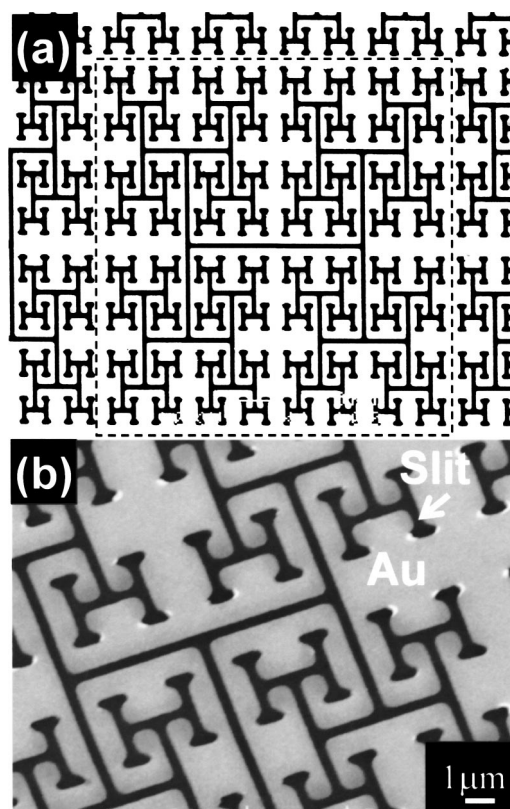


FIG. 1. (a) shows SEM image of the fractal slit pattern; and (b) is an enlarged part of (a). The slits are 0.5  $\mu\text{m}$  wide and forms a space-filling-curve type fractal pattern generated by the repeated affine transformations of an H-shaped mother element, with the longest line measuring 27.8  $\mu\text{m}$ . The geometrical details can be found in Ref. 11. The dimension of the whole sample is  $15 \times 15 \text{ mm}^2$ , which is composed of periodically replicated fractal units ( $55.6 \times 55.6 \mu\text{m}^2$  with nine fractal levels).

<sup>a)</sup>Electronic mail: phwen@ust.hk

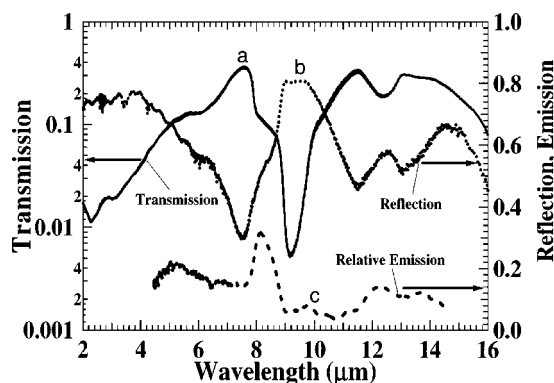


FIG. 2. Curves (a), (b), and (c) show the infrared transmission, reflection, and emission of the fractal sample with 0.5  $\mu\text{m}$  slits on the gold film.

plicated fractal units. The infrared reference sample has a square lattice array of 0.5  $\mu\text{m}$  diameter holes, at 2  $\mu\text{m}$  center-to-center distance, in a 100-nm-thick gold film on silicon wafer.

The infrared spectra were measured using a Bruker IFS66 Fourier transform spectrometer (FTS). Air and a thick smooth gold film were used as the references for transmission and reflection, respectively. The collecting angle was  $\sim 20^\circ$  for both transmission and reflection. For the emission spectra, a smooth and highly reflective aluminum sheet, with a 3 mm diameter hole, was placed in front of the sample as the aperture, and a ZnSe lens of 75 mm focal length was used to collimate the emission radiation to the entrance port of the FTS. For each fractal sample, the emission spectra were taken from a gray body (reflectivity  $< 5\%$ )  $E_B$ , the sample  $E_S$ , and a gold film (reflectivity = 98%)  $E_G$ , all heated to 150  $^\circ\text{C}$ . The relative emission of the sample was then determined by  $(E_S - E_G)/(E_B - E_G)$ . A wire grid polarizer was used for polarization selection.

Figure 2 shows the transmission (curve a), reflection (curve b), and relative emission (curve c) of the sample at normal incidence. For the transmission spectrum, there is a stop band (dip) centered at 9.2  $\mu\text{m}$ , with a minimum transmission of 0.5%. There are also two passbands centered at 7.5 and 11.5  $\mu\text{m}$ , respectively, with a maximum transmission of about 36%. Since the bare silicon substrate was measured to have 40% transmission, the transmission of the fractal slit pattern alone could be significantly higher than 36%. The reflection spectrum is seen to display peak(s) and dip(s) in perfect match to the transmission stop and passbands. Moreover, as shown in the upper panel of Fig. 3, there is almost

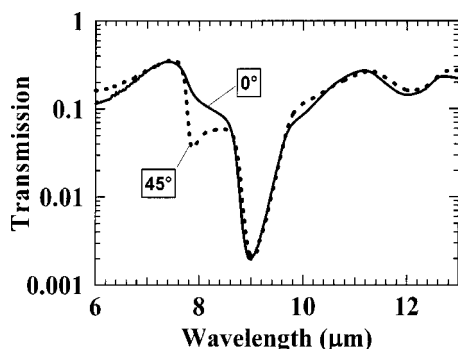


FIG. 3. Stop bands with two different incident angles are shown.

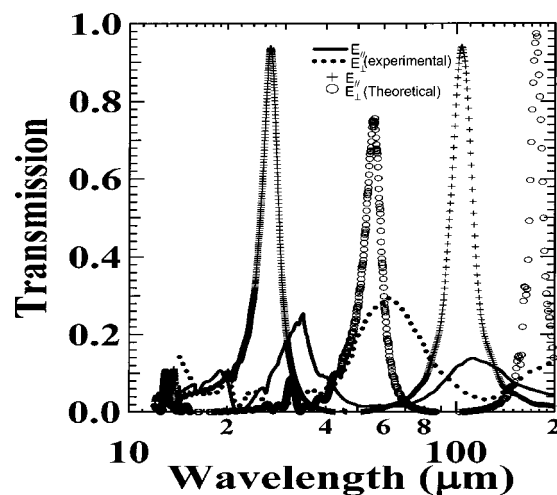


FIG. 4. Transmittance measured in far-infrared regime. Here  $E_{\parallel}$  is defined as the EM wave polarization with the electric field parallel to the shortest slits of the fractal pattern, while  $E_{\perp}$  is rotated to  $90^\circ$ . Finite-difference-time-domain simulations, assuming perfect metal boundary conditions, are shown for comparison.

no shift for the stop band at 9.2  $\mu\text{m}$  as the incident angle was varied from  $0^\circ$  to  $45^\circ$ , while maintaining the electric field to be perpendicular to the plane of incidence. The relative emission spectrum also shows a peak around the same wavelength where the reflection is minimum and a drop where the reflection is a maximum.

We have fabricated a reference sample consisting of 0.5  $\mu\text{m}$  diameter circular holes on an Au film with equal void-to-metal area ratio as the fractal slits. The reference sample is expected to display classic diffraction limit transmission, since the metal surface plasma frequencies are much higher than the IR radiation. The measured transmission was found to be  $< 0.01\%$  for all the relevant infrared frequencies, which is 3000 times lower than the transmission peak of the fractal slits. The underlying physics of transmission enhancement is due to the electromagnetic resonances induced in the slits. We have previously observed pass and stop bands in metallic fractal patterns deposited on dielectric plates.<sup>11</sup> The current samples are inverted structures scaled down to IR regime. We believe that the physics underlying the stop and passbands in the IR samples and its complementary (geometrically inverted) counterparts in the microwave regime share the same origin. These slit resonances are related by the Babinet's principle<sup>12</sup> to the geometric resonances of its complement, (the metallic fractal where the metallic part forms the fractal pattern), whereby the roles of the transmission and reflection are reversed for the two complementary structures, simultaneous with a  $90^\circ$  rotation in polarization.

The transmittance in the far-infrared regime was measured with the same sample and the results are shown in Fig. 4. We observe from experiment that 25% and 14% transmissions at wavelength of 34 and 111  $\mu\text{m}$  for the case of  $E_{\parallel}$ , while 29% transmission at wavelength 62  $\mu\text{m}$  for the case of  $E_{\perp}$ . Again, because the substrate transmission is at most 40%, the transmission of the fractal patterns alone are significantly higher than these values. For those cases, the infrared wavelengths are much longer than that of slits etched on the gold plate. In Fig. 4, we show for comparisons finite-difference-time-domain (FDTD) simulation results, which

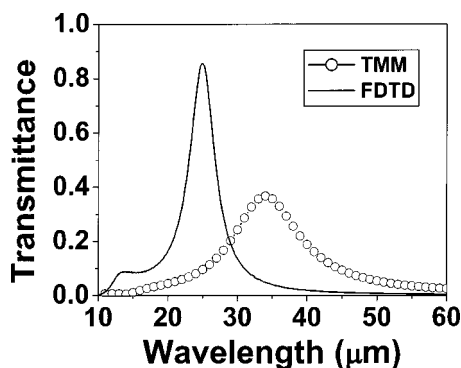


FIG. 5. Comparison of FDTD calculated results with TMM calculated results for a two-level fractal pattern. The first level line is  $2.5 \mu\text{m}$ , line width is  $0.5 \mu\text{m}$ , film thickness is  $0.1 \mu\text{m}$ .

show a series of high transmittance in qualitative agreement with experimental measurement. Due to computing power limitations, the simulation differs from experimental setup in two aspects: (i) Perfect metal boundary conditions are assumed and (ii) the Si substrate is approximated by a nonabsorbing  $\epsilon = 12$  medium, and is taken to be  $3 \mu\text{m}$  for  $\lambda > 45$  and  $1 \mu\text{m}$  for  $\lambda < 45 \mu\text{m}$ . These approximations tend to push up the pass frequencies and exaggerate transmittance. From the simulation, we can trace the high transmittance to the resonances of EM modes in the slits of the entire fractal unit array. Fractal-like structures can, in principle, support a multiple of long-wavelength resonances.<sup>11</sup> We note from Fig. 4 that the FDTD simulations reproduce the salient features of the experimental spectrum, but agreement is not quantitative because FDTD does not take into account of dispersion and absorption. In Fig. 5, we compare FDTD results with transfer-matrix (TMM)<sup>13</sup> results for a simpler system which has two-levels of slits. TMM can handle dispersion and absorption, except that the convergence and stability issues limit its application to a fractal with small number of levels.

The comparison in Fig. 5 shows that when dispersion and absorption is properly taken into account, the transmittance drops to about 30% and there is downshift in frequency, which explains the discrepancy between FDTD simulation and the measured spectra.

In summary, we have shown that fractal metal slits with submicron width exhibit strong pass and stop bands in the infrared regime, due to resonances. Strong frequency selective transmission enhancements are observed, where the wavelengths are 10–200 times the slit width. The characteristics of these bands are almost independent of the incidence angle of the IR radiation.

This work was supported by RGC Hong Kong through Grant Nos. N\_HKUST025/00, HKUST6154/99P, and CA02/03.SC01.

- <sup>1</sup>E. Yablonovitch, Phys. Rev. Lett. **58**, 2059 (1987).
- <sup>2</sup>S. John, Phys. Rev. Lett. **58**, 2486 (1987).
- <sup>3</sup>J. D. Joannopoulos, R. D. Meade, and J. Winn, *Photonic Crystals* (Princeton University, Princeton, NJ, 1995).
- <sup>4</sup>L. Zhang, R. F. Jimenez Broas, N. G. Alexopolous, and E. Yablonovitch, IEEE Trans. Microwave Theory Tech. **47**, 2059 (1999).
- <sup>5</sup>J. A. Porto, F. J. Garcia-Vidal, and J. B. Pendry, Phys. Rev. Lett. **83**, 2845 (1999).
- <sup>6</sup>H. E. Went, A. P. Hibbins, and J. R. Sambles, Appl. Phys. Lett. **77**, 2789 (2000).
- <sup>7</sup>Y. Takakura, Phys. Rev. Lett. **86**, 5601 (2001).
- <sup>8</sup>F. Yang and J. R. Sambles, Phys. Rev. Lett. **89**, 063901 (2002).
- <sup>9</sup>T. W. Ebbesen, H. J. Lezec, H. F. Ghaemi, T. Thio, and P. A. Wolff, Nature (London) **391**, 667 (1998).
- <sup>10</sup>L. Martin-Moreno, F. J. Garcia-Vidal, H. J. Lezec, K. M. Pellerin, T. Thio, J. B. Pendry, and T. W. Ebbesen, Phys. Rev. Lett. **86**, 1114 (2001).
- <sup>11</sup>W. Wen, L. Zhou, J. Li, W. Ge, C. T. Chan, and P. Sheng, Phys. Rev. Lett. **89**, 223901 (2002).
- <sup>12</sup>B. A. Munk, *Frequency Selective Surfaces, Theory and Design* (Wiley, New York, 2000).
- <sup>13</sup>P. M. Bell *et al.*, Comput. Phys. Commun. **85**, 306 (1995). Dielectric function of Au is taken from M. A. Ordal *et al.*, Appl. Opt. **22**, 1099 (1983).